NACA TN 2120

CASE FILE COPY

NATIONAL ADVISORY COMMITTEE FOR AERONAUTICS

TECHNICAL NOTE 2120

DEVELOPMENT AND PRELIMINARY INVESTIGATION OF A METHOD OF

OBTAINING HYPERSONIC AERODYNAMIC DATA BY FIRING

MODELS THROUGH HIGHLY COOLED GASES

By Harold V. Soule and Alexander P. Sabol

Langley Aeronautical Laboratory
Langley Air Force Base, Va.

NACA

Washington

July 1950

NATIONAL ADVISORY COMMITTEE FOR AERONAUTICS

TECHNICAL NOTE 2120

DEVELOPMENT AND PRELIMINARY INVESTIGATION OF A METHOD OF

OBTAINING HYPERSONIC AERODYNAMIC DATA BY FIRING

MODELS THROUGH HIGHLY COOLED GASES

By Harold V. Soule and Alexander P. Sabol

SUMMARY

A method of investigating hypersonic aerodynamic phenomena by firing simple symmetrical models at high velocity through a very cold gas having a low sonic velocity has been developed. The high model velocities were produced in a commercially available gun, whereas the low acoustical velocities were attained by liquid–nitrogen cooling of the test gas.

Schlieren photographs and "focused" shadowgraphs were taken of cylindrical models having conical forebodies with apex angles of 30°, 45°, and 60°. In these tests a short–duration light source was used; a rotating–mirror camera was added in order to obtain sharp–focused shadowgraphs.

The conical shock angles were measured at a Mach number of about 6.7 and were found to agree with values computed theoretically within the limits of the accuracy of the present system.

INTRODUCTION

Aerodynamic data at hypersonic Mach numbers are at present so limited that the aerodynamic characteristics of high Mach number bodies must be based almost entirely upon aerodynamic theory, the validity of which has not been adequately demonstrated experimentally even for elementary flows. Progress has been made in extending the Mach number range of wind–tunnel, rocket–flight, and aeroballistic techniques for use in the study of hypersonic phenomena. However, the problems encountered in hypersonic wind tunnels and rocket flights make it desirable to find a comparatively simple, inexpensive, and expedient technique which may be used for at least an initial exploration of hypersonic aerodynamics.

Firing ranges have long been used to study exterior ballistics. The application of data from the ballistics range to the design of aircraft is discussed in reference 1. Recent improvements in technique have substantially increased the Mach number range of ballistic research by the use of high projectile velocities (reference 2). Use of dense gases in which the speed of sound is relatively low has also increased the Mach numbers attainable.

This investigation was undertaken to determine the feasibility of extending the ballistic technique to hypersonic Mach numbers by reducing the gas temperature, and thus decreasing the velocity of sound in the gas. The resulting comparatively low and easily changeable model velocity required to obtain a high Mach number, together with the adjustable density, would permit the attainment of a wide range of Mach and Reynolds numbers and, from sharp photographs of the flow phenomena from which shock-wave shape could be measured, the aerodynamic characteristics of a body in free flight could be determined.

A commercially available, .220-caliber high-velocity gun was used to obtain model velocities of the order of 4200 feet per second. Liquid nitrogen was used to cool a low-temperature chamber and the gas therein, and thus produce the low acoustical velocities. Mach numbers of the order of 6.7 and a Reynolds number range up to 5×10^6 based on the model diameter of 0.224 inch were obtained in nitrogen. Both schlieren and focused shadowgraphs of the conical shock patterns were taken.

APPARATUS

Description and operation.— The method used to obtain hypersonic phenomena consisted of firing a model at high velocity through a chamber filled with nitrogen gas in which the velocity of sound had been reduced by cooling. Photographs in figure 1 show the relative size of the component parts of the hypersonic apparatus, whereas figure 2 indicates the general arrangement of this apparatus. The model was fired from rifle A through the low-temperature chamber E and was stopped by the sand trap G. Twin photocells operate the interval timer H, which records the time required for the model to traverse the distance between the cells. The optical system in figure 2(b) was used to obtain focused shadowgraph pictures. A similar system without the rotating-mirror camera was employed to obtain schlieren photographs.

Low-temperature chamber.— The chamber for maintaining, at a low temperature, the gas in which the test is performed is shown schematically

in figures 2(a) and 2(b) and in a dimensioned perspective drawing in
figure 2(c). This low-temperature chamber is composed of two concentric
cylindrical compartments. The cooled test gas was contained within the
inner compartment, the flat ends of which are windows and the curved
sides of which are of double-wall construction forming a cooling jacket.
This inner compartment and its jacket were constructed of type 304 stain-
less steel, which does not tend to become too brittle at low temperatures.
To minimize cooling problems, the inner chamber and its cooling jacket
were enclosed within an outer cylindrical chamber of cold-rolled steel as
shown in figures 2(a) and 2(b).

Reduction of heat transfer from the atmosphere to the gas in the
inner compartment was accomplished by maintaining a vacuum outside the
cooling jacket. The facing surfaces of these inner and outer compart-
ments were coated with aluminum foil and portions of the outer windows
were silvered to reduce heat radiation. Baffles were installed in the
horizontal model passage tubes to reduce thermal currents within the
test medium. To maintain a low pressure within the inner test compart-
ment, caps, together with neoprene gaskets, were used to hold a
0.0015-inch brass pressure seal in place. Outside the low-temperature
enclosure, the bullet passage tubes projected into wooden gas containers
through which vaporized nitrogen passed. (See M in figs. 2(a) and 2(b).)
When the pressure seal was punctured, the dry nitrogen gas in these con-
tainers entered the inner compartment; thus, the flow of atmospheric air
into the test chamber was minimized.

Moisture condensation on the windows of the outer compartment was
removed between tests by streams of warm air directed against the outer
surfaces. All the low-temperature-chamber windows were of selected plate
glass. At these low temperatures a vacuum seal for the inner windows
consisting of a steam-boiler gasket material coated with a silicone-base
putty was found to be very satisfactory.

The method of supplying and controlling coolant flow into the
chamber is illustrated in figure 2(a). This system used a source of
dry gas under slight pressure to force liquid nitrogen from a Dewar
flask L into the cooling jacket. The nitrogen evaporated at atmospheric
pressure. Cooling was performed at a uniform slow rate to avoid uneven
thermal contractions which would destroy the vacuum seals.

Temperature measurements were taken at eight stations close to the
model's trajectory in the test region with copper-constantan junctions
of 36-gage wire (fig. 2(a)). The reference junctions were held at
standard conditions and thermal electromotive force was measured by a
precision potentiometer. Thermocouples were calibrated to standard
temperatures with a resistance platinum thermometer which had been
calibrated by the Bureau of Standards. The recording accuracy was
within 1^O at temperatures of -300° F.

Model propulsion system.— The gun used to propel the models was a
commercially available .220-caliber Winchester, Model 70, Swift rifle.
This gun has a land's diameter of 0.220 inch and fires a 0.224-inch-
diameter model. The rifling of this gun makes one turn in 14 inches.
The gun was positioned 6 feet from the test area, and all intervening
apparatus was alined by boresighting the barrel. Reloading practices
outlined in reference 3 were followed in the making of propellent charges
which would produce a model velocity of about 4200 feet per second.
Cylindrical models with conical forebodies, shown in figure 3, were
machined from copper for these tests.

Optical arrangements.— To obtain accurate aerodynamic measurements
of the shock-wave pattern existing about the model necessitated photo-
graphing a model with no apparent motion. Two approaches to this problem
were made with optical arrangements resembling that of figure 4: one
employed a short-duration spark-light source with schlieren optics; and
the other, a focused shadowgraph system, combined a longer-duration
spark with a rotating-mirror camera. To minimize image blurs in the
schlieren photographs which were made without the rotating-mirror camera,
the effective light exposure was reduced to a measured 0.2 to 0.3 micro-
second. With a one-sixth image reduction, difficulty was encountered in
obtaining photographs of sufficient density, and motion of the image
during exposure was apparent. Therefore, the use of a focused shadow-
graph system with a rotating-mirror camera and a longer-duration spark
was adopted for most of the tests.

Figure 4 is a diagram of the focused shadowgraph system which is
similar to the one described in reference 4. Fundamentally, this focused
shadowgraph system is quite similar to a single-traverse conventional
schlieren system. The second parabolic mirror and the lens constitute
a photographic system for which the plane BB' appears fully illuminated.
However, in the plane CC' of the film conjugate to DD', the illumination
is not uniform and demonstrates the same shadowgraph pattern as if the
film were placed at DD'; that is, the rays diverging from BB' identically
represent the rays diverging from AA'.

A point source of light having a duration of 1.0 to 1.5 microseconds
was created by a discharge from a low-inductance condenser (fig. 5(c)).
The spark gap consisted of tungsten electrodes shielded by quartz tubing.
Light was rendered parallel through the chamber by an $f/6$, $29\frac{1}{2}$-inch
focal length, first-surface parabolic mirror. The light beam was
received by a second mirror, which, with a 14-inch focal-length lens,
formed an image of the source on a rotating mirror located within a
camera. The camera unit consisted of a four-sided, fully silvered mirror
mounted on an air-driven shaft and a film support extending 180° about
the axis of the shaft. With this unit the image of the model appeared

on the film at one-third full scale. Precise matching of the mirror
rotational speed to the model velocity was found unnecessary.

By use of a reference reticule, it was found that the alinement of
the optical components needed no correction for the range of accuracy
of the present equipment. The reticule was positioned in the cooled
test chamber and a glass-plate negative was held near the chamber per-
pendicular to the parallel light rays. A shadowgraph of the true orienta-
tion of the reticule was thus obtained. Similar photographs of the
reticule were then taken uniformly spaced on the film in the camera by
flashing the light source for fixed mirror angles. The true reticule
pattern was compared with those which were positioned at the random
locations of the model image.

Electronic components.— The electrical instruments used to determine
the average velocity of the model between stations B were separated by a
space of 8 feet $\pm\frac{1}{16}$ inch and were symmetrically located about the chamber.
Photoelectric cells at points B were activated by the model, which sent
elapsed signals to a gated chronograph. Identical delays in signals
reaching the counter from both cells were apparent after the model's
penetration into the detecting light beam. The chronograph possessed a
base counting frequency of 1.6 megacycles which, when combined with the
linear measurement, gave an accuracy of ±0.2 percent in determining the
average velocity.

Three phototube detectors of the same design were used for the
bullet location and the chronograph gating. These detectors consisted
of a vacuum phototube, RCA 929, and a light source (fig. 5(a)) mounted
in the same chassis. A positive-voltage pulse is provided by the photo-
tube circuit when the light beam is interrupted. This pulse is capaci-
tively coupled to a pulse-generator circuit, a single-shot multivibrator,
and gives, therefore, a large output independent of the amplitude of the
phototube signal and coincident with it for operation of other equip-
ment. A lamp using filtered direct-current power supply minimized any
possible effects of light ripple. The optical system was arranged to
focus at a point midway between the phototube and the light source.

The optical and electrical parts of this unit have been designed to
minimize delay and variation in delay in reaction to passage of the
bullet. By increasing the sensitivity to maximum or, in more critical
cases, by matching the sensitivities of the units, the firing point may
be set to within a small fraction of the bullet length to obtain maximum
accuracy in the velocity reading. Crystal diodes were introduced in the
output circuit to eliminate cross-coupling between the two units associ-
ated with the chronograph.

The timing unit diagrammed in figure 5(b) provides adjustable delay
of 240 to 400 microseconds to operate the spark when the bullet has
reached the center of the cold chamber and consists of a thyratron input
circuit, a timer, and a low--impedance output circuit. The thyratron
circuit provides a pulse of constant amplitude independent of the signal
and acts as a lockout to prevent accidental refiring of the spark. A
biased diode is included between the thyratron and the timer circuit to
eliminate the low--amplitude noise which accompanies thyratron conduction
and which could affect the accuracy of the timing. The timing circuit
is a cathode--coupled, single--shot multivibrator, highly stable in spite
of plate--voltage variation. This circuit is followed by a differ--
entiator, an amplifier, and a cathode follower, which provide an output
pulse of large amplitude at a low impedance coinciding with the end of
the single--shot multivibrator pulse. In use, the only variation in
placing of the bullet in the field of view was due to the difference
between bullet velocities.

RESULTS AND DISCUSSION

For convenience during these preliminary tests, nitrogen was used
instead of air. However, other types of gases could have been used with
slight modifications to the apparatus. If liquid nitrogen is used to
cool room air, the nitrogen boils at atmospheric pressure at a tempera--
ture which makes it necessary to keep the pressure within the chamber
below 0.5 atmosphere at all times in order to keep the oxygen from con--
densing out on the windows and forming a fog in the chamber. This
difficulty might be overcome by the use of liquid--oxygen coolant or by
boiling nitrogen at a sufficiently high pressure and temperature.

Figure 6 shows the location of the phenomena on the nitrogen phase
diagram. In this diagram, the shock phenomena lie to the right of the
liquefaction line for nitrogen. The initial condition of 200 millimeters
of mercury or 0.26 atmosphere pressure was used because it appeared to
give the best detail in the pictures with the present optical arrangement.
Below about 0.025 atmosphere, the density change across the shock was
found to be so slight that it could not be recorded satisfactorily. At
1.0 atmosphere, the shock intensity was so great that flow details about
the model were obscured.

The initial temperature shown in figure 6 was determined by the
heat--conducting characteristics of the equipment and the boiling point of
commercially available liquified nitrogen. This liquid, when vaporized,
was carbon--dioxide and water--vapor free.

Mach number was determined by dividing the measured velocity of
the model by the velocity of sound corresponding to the recorded pressure

and average gas temperature. The values of the speed of sound shown in
figure 7 were computed, whereas the two values indicated by symbols were
extrapolated from experimental data in reference 5. Figure 8 presents
the temperatures and velocities necessary to obtain a given Mach number.
The limiting upper-chamber pressure in the low-temperature regions is
established by the dew point of nitrogen.

A schlieren photograph of a model traveling at a Mach number of 6.8
is shown as figure 9. This 30° conical model is traveling from right
to left with a velocity of about 4200 feet per second. The symmetrical
appearance of the model and shock-wave pattern indicates that there is
a minimum of yawing in the vertical plane, and the absence of rounding
of the rear of the model profile indicates that the yaw in the horizontal
plane was not excessive. In this photograph, the light line across the
cone tip and the very dark spots outside the wake of the projectile are
caused by defects in the windows and film and are not associated with the
flow field. It was noted that, as predicted in theory, the conical shock
continues for some distance behind the cone-cylinder junction before
starting to bend as a result of the interaction of the shock and expan-
sion waves. A clearly defined wake appears to start some distance behind
the body. Along the cylinder portion of the body, there appears to be
a wide turbulent region which may, to some extent, have been caused by
rifle engraving on the model.

Figures 10(a), 10(b), and 10(c) are focused shadowgraphs of conical
models traveling from right to left through the low-temperature chamber
at about 4200 feet per second. In these shadowgraphs, all stationary
objects appear to have motion, whereas the model outline appears station-
ary because of the sweep of the image reflected from the rotating mirror.
Although figure 9 shows much more detail in the flow than the shadow-
graphs of figure 10, the shock profiles are more sharply defined in
figure 10 and may, therefore, be measured with greater accuracy. Since
only the shock-wave profile is measured, no correction factors are neces-
sary for internal-shock light refraction.

It was found that models having small cone angles usually tended
to yaw considerably, with the amount of yaw increasing with decreasing
cone angles. For this reason, 45° and 60° conical models similar to
those shown in figure 3 were used to check existing theory.

In figure 10(b) the dark object in the lower part of the shadow-
graph is the profile of a shielded thermocouple. The black line across
the shock in figure 10(c) is caused by a defect in the film.

In all the shock photographs there appears to be a lack of detail
at the cone vertex. Since several factors are involved — including the
optical system, the high stagnation temperatures and pressures, and
possible slight model imperfections — a satisfactory analysis of this

effect has not been completed. In the shock-angle determinations, measurements were made from a point behind the cone vertex to a point opposite the cone-cylinder junction.

Parallel-light shadowgraphs of model profiles were made prior to their firing and were recorded on lantern-slide glass plates from which cone-angle measurements were taken. Shock-wave angles were determined directly from the original negatives. In both cases, several points along the generatrix of the cone or shock wave were measured from a magnified view by use of a toolmaker's microscope; the average angle was determined by the method of least squares.

The image size had to be reduced about one-third so that the photograph of the model would contain sharp definition. This size reduction gave a measurable shock length of about 0.1 inch, which could be accurately read to 0.001 inch. Increasing the measurable shock length by improving the optical equipment or increasing the model diameter would, of course, result in much better accuracy if the conical shock-wave-angle measurements could still be read to 0.001 inch.

To obtain theoretical values of the conical shock-wave angle for higher Mach numbers than could be obtained from references 6 and 7, the curves in figures 11(a) and 11(b) were computed by use of reference 8. A value of 1.405 for γ (nondimensional ratio of specific heat at constant pressure to specific heat at constant volume) was used to compute these shock angles, since this was the mean value of γ for the pressures and temperatures involved. The temperature gradient within the test chamber amounted to about a measured 30° F between the top and bottom banks of thermocouples so that the over-all accuracy of the Mach number determination is about ±4.5 percent. Thermal currents within the bullet passage tubes and currents caused by the warm inner chamber windows appeared to have caused most of the temperature gradient within the test chamber. This temperature gradient can be reduced considerably by alteration of the chamber design.

From the slopes of the curves in figures 11(a) and 11(b), the shock angle θ_w is seen to be almost directly dependent upon the cone angle θ_s and, therefore, much more accuracy is necessary in reading the cone angles than is necessary in determining Mach numbers. The ±4.5-percent Mach number accuracy gives a 0.20° difference in the computed shock angle, whereas only a ±0.22-percent deviation in the measurement of a 45° cone angle will give about the same computed shock-wave-angle difference.

The results of several runs made in nitrogen are given in table I. All these models had about the same Mach and Reynolds numbers. The shadowgraphs for these tests were similar in appearance to figures 10(b) and 10(c). At a Mach number of 6.7, the experimental and computed shock-wave angles agreed within the limits of accuracy of the present equipment. These limits of accuracy are discussed in the preceding paragraphs.

In general, change in Mach number could be more easily obtained in this apparatus by changing the velocity of the model than by changing the chamber temperature. It is possible, with the proper selection of pressures and temperatures, to use gases other than nitrogen in this apparatus. The use of dense gases offers the possibility of obtaining appreciably higher Mach numbers than were obtained in the present investigation.

CONCLUSIONS

The following conclusions are based upon the development and preliminary investigation of a method of obtaining hypersonic aerodynamic data by firing models through highly cooled gases:

1. The practicability of increasing the test Mach number of a model by refrigeration of the test medium is established.

2. At Mach numbers of approximately 6.7 obtained in these tests, the shock angles computed by using a constant value of specific heat ratio of 1.405 agreed with experimental results.

Langley Aeronautical Laboratory
    National Advisory Committee for Aeronautics
        Langley Air Force Base, Va., April 7, 1950

REFERENCES

1. Charters, A. C.: Some Ballistic Contributions to Aerodynamics. Jour.
      Aero. Sci., vol. 14, no. 3, March 1947, pp. 155-166.

2. McMillen, J. H., and Kramer, R. L.: Method for Shooting Spheres at
      Velocities of Seven-Thousand Feet per Second. Naval Ordnance Lab.
      Memo. 9188, U. S. Naval Gun Factory, July 23, 1947.

3. Sharpe, Philip B.: Complete Guide to Handloading. Third ed.,
      Funk & Wagnalls Co., 1949.

4. Winckler, John: The Mach Interferometer Applied to Studying an
      Axially Symmetric Supersonic Air Jet. Rev. Sci. Instr., vol. 19,
      no. 5, May 1948, pp. 307-322.

5. Claitor, L. C., and Crawford, D. B.: Thermodynamic Properties of
      Oxygen, Nitrogen and Air at Low Temperatures. Preprints of Papers
      Contributed by A.S.M.E. Special Res. Committee on Properties of
      Gases and Gas Mixtures (Annual Meeting, N. Y., Nov. 28-Dec. 3, 1948),
      Towne Sci. School, Univ. Pa., Nov. 19, 1948, pp. 3-45.

6. Staff of the Computing Section, Center of Analysis (Under Direction
      of Zdeněk Kopal): Tables of Supersonic Flow around Yawing Cones.
      Tech. Rep. No. 3, M.I.T., 1947.

7. Staff of the Computing Section, Center of Analysis (Under Direction
      of Zdeněk Kopal): Tables of Supersonic Flow around Cones. Tech.
      Rep. No. 1, M.I.T., 1947.

8. Ferri, Antonio: Elements of Aerodynamics of Supersonic Flows. The
      Macmillan Co., 1949.

TABLE I.— RESULTS FOR 60° AND 45° CONES

Test	Temperature (°F abs.)	Velocity (ft/sec)	Mach number	Cone half-angle (deg)	Measured shock half-angle (deg)	Computed shock half-angle (deg)	Difference between measured and computed shock angles (deg)	Figure
				60° cones				
1	158	4206	6.7	30.2	35.1	34.8	0.3	10(c)
2	158	4130	6.6	30.2	34.6	34.8	–.2	-----
3	159	4201	6.7	30.0	34.4	34.6	–.2	-----
4	159	4162	6.6	30.1	35.1	34.7	.4	-----
5	161	4317	6.9	30.1	34.5	34.6	–.1	-----
				45° cones				
6	156	4108	6.6	22.6	27.1	26.5	0.6	10(b)
7	156	4226	6.8	22.5	26.5	26.3	.2	-----
8	156	4194	6.7	22.4	26.5	26.2	.3	-----
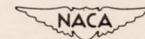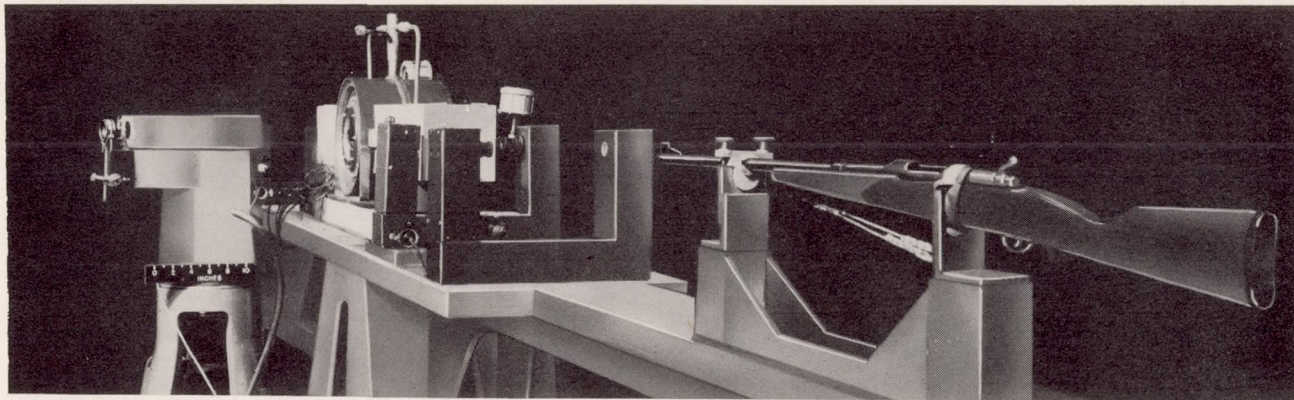
(a) General arrangement.
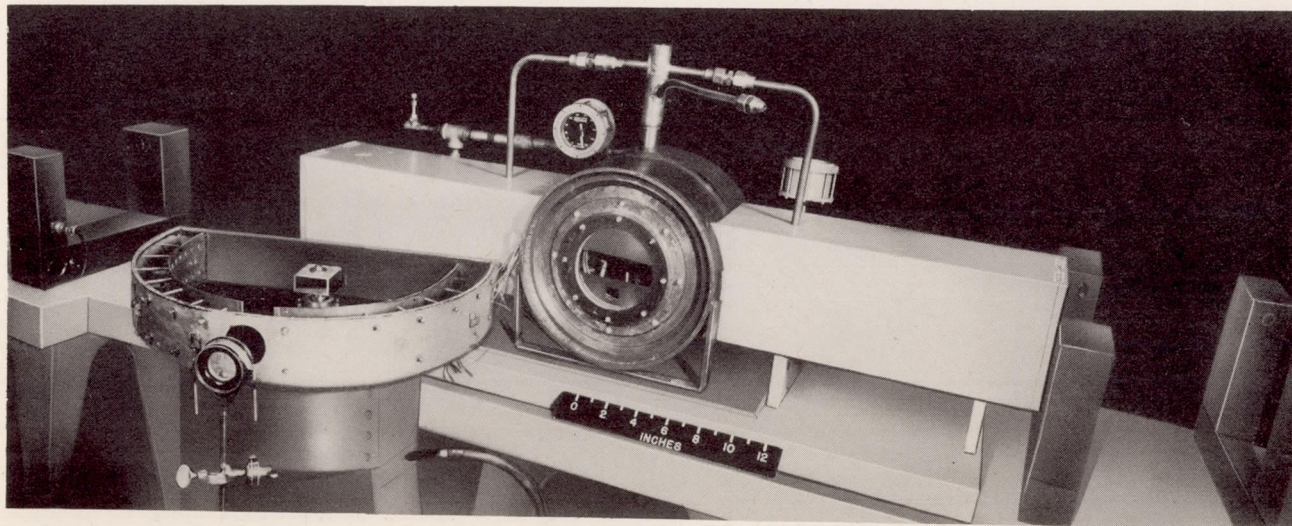
(b) Side view.
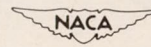
L-64872

Figure 1.- Photographs of the hypersonic apparatus.
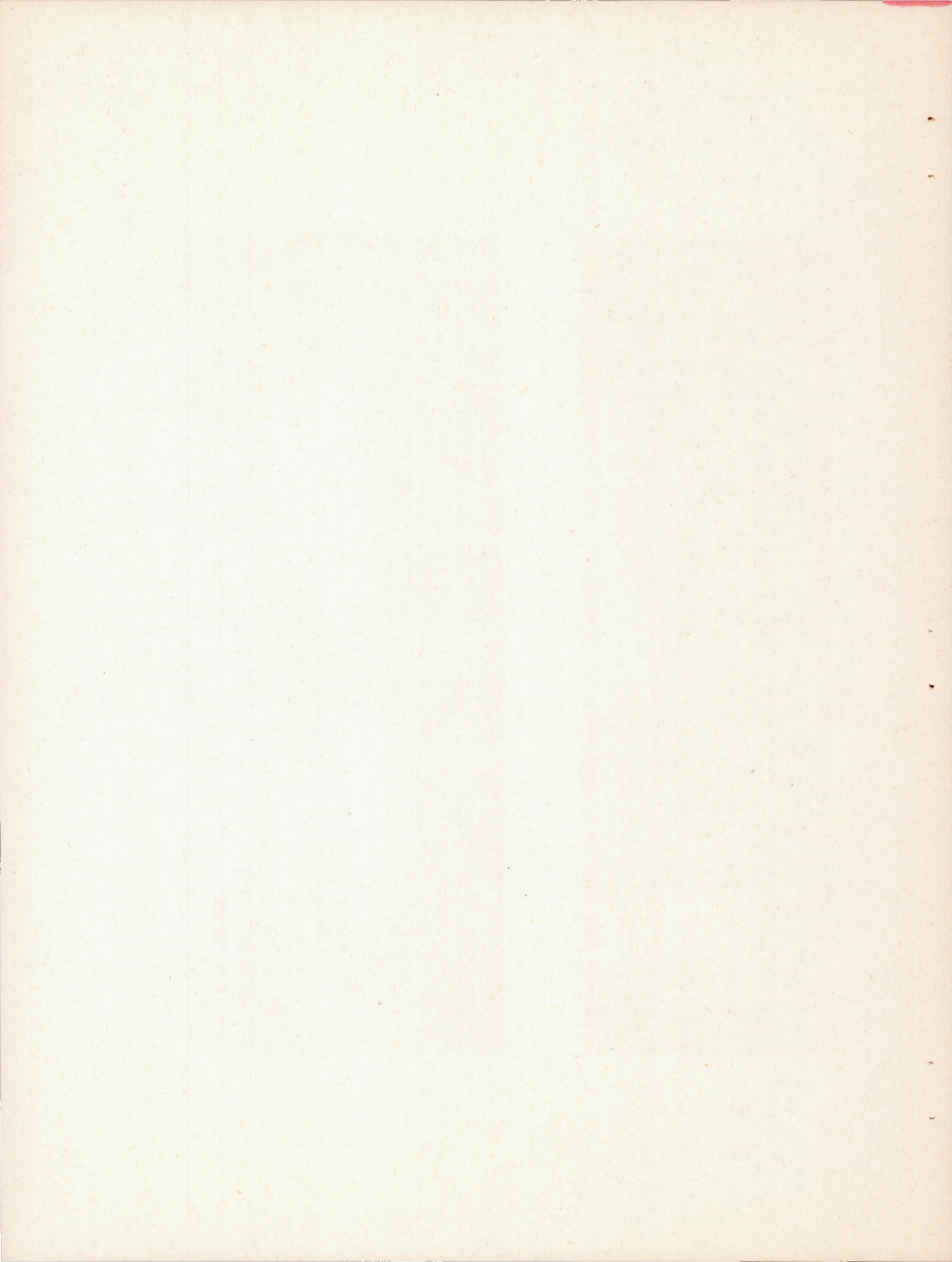
A - .220-caliber rifle
B - Photoelectric cell
C - To vacuum pump
D - Baffles
E - Low-temperature chamber
F - Spark trigger cell
G - Sand trap
H - Interval timer
I - N_2 gas bottle
J - Pressure regulator
K - Pressure gage
L - Dewar flask - liquid N_2
M - N_2 gas
N - Silvered outside windows
O - Unshielded thermocouple
P - Clear window
Q - Shielded thermocouple
R - Flight path
S - Reference reticule
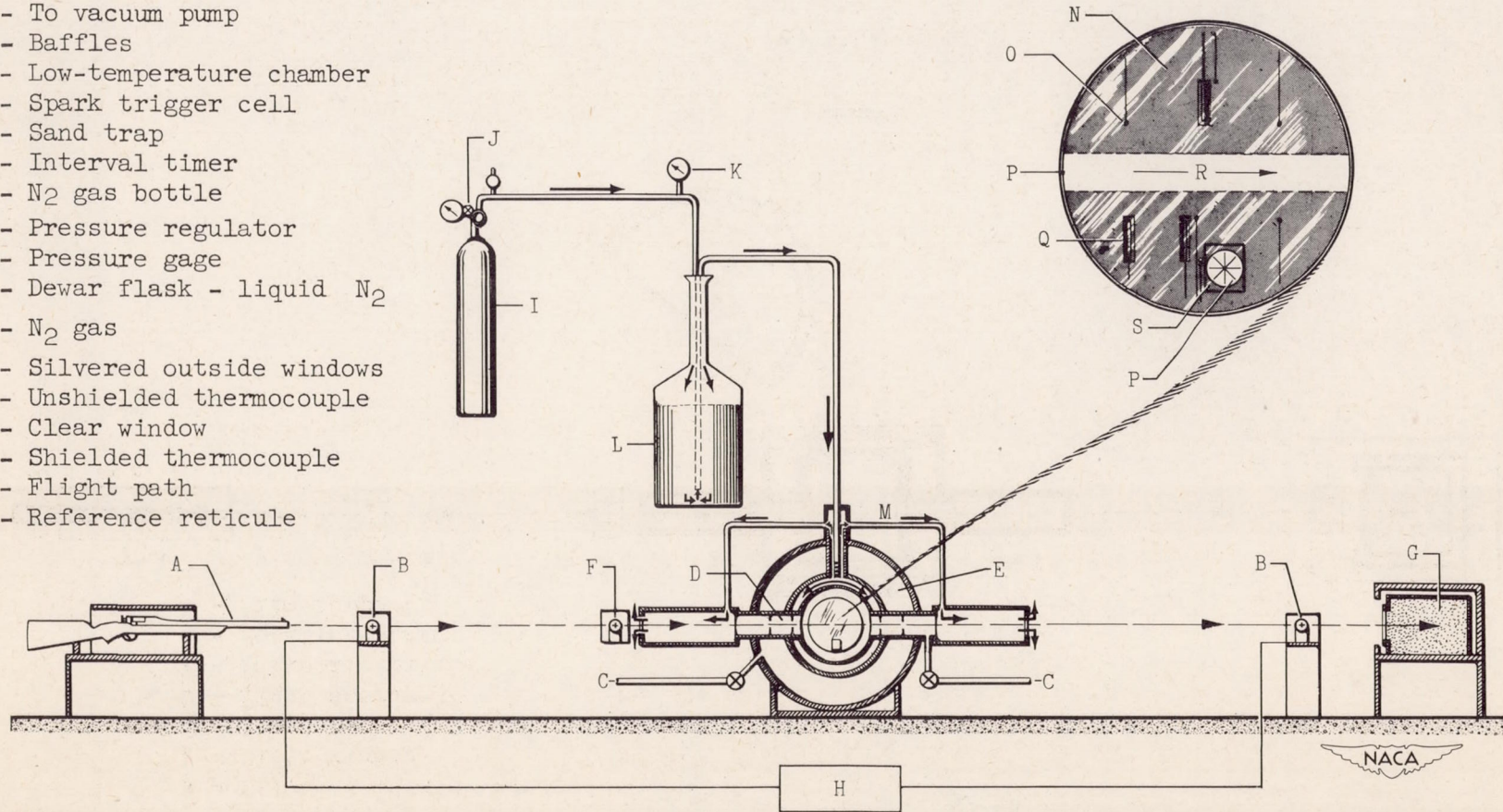
(a) Side view.

Figure 2.- Schematic diagram of the apparatus.
(Not to scale.)

A - .220-caliber rifle
B - Photoelectric cell
F - Spark trigger cell
M - N$_2$ gas
N - Silvered outside window
P - Clear window
T - Pressure seal
U - Light source
V - Parabolic mirror
W - Rotating mirror
X - Film support
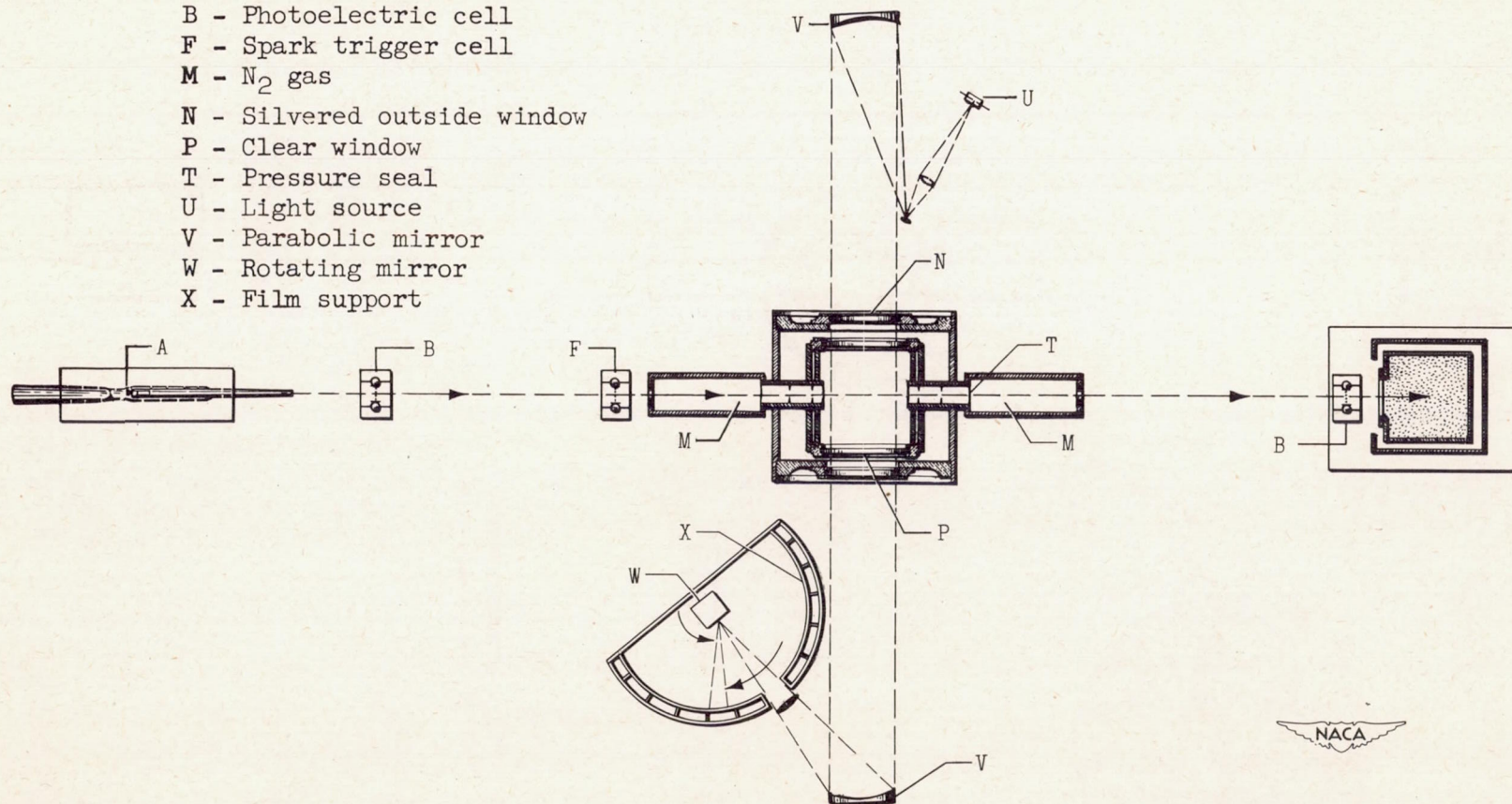
(b) Plan view.

Figure 2.- Continued.

$1\frac{1}{4}$" O.D.

Wooden-gas-container outline

$5\frac{1}{2}$"D. Window

$2\frac{1}{4}$" O.D.

$12\frac{3}{4}$"O.D.

NACA

$10\frac{1}{2}$"
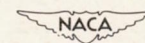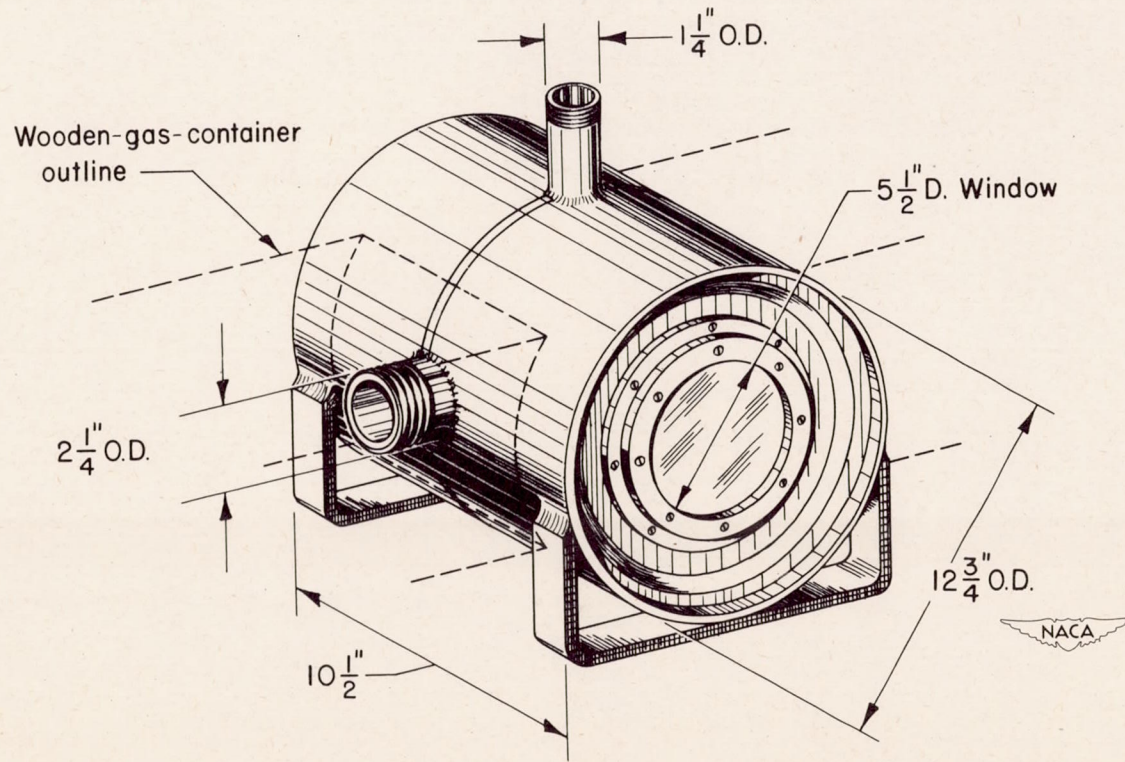
(c) Low-temperature chamber dimensions.

Figure 2.- Concluded.
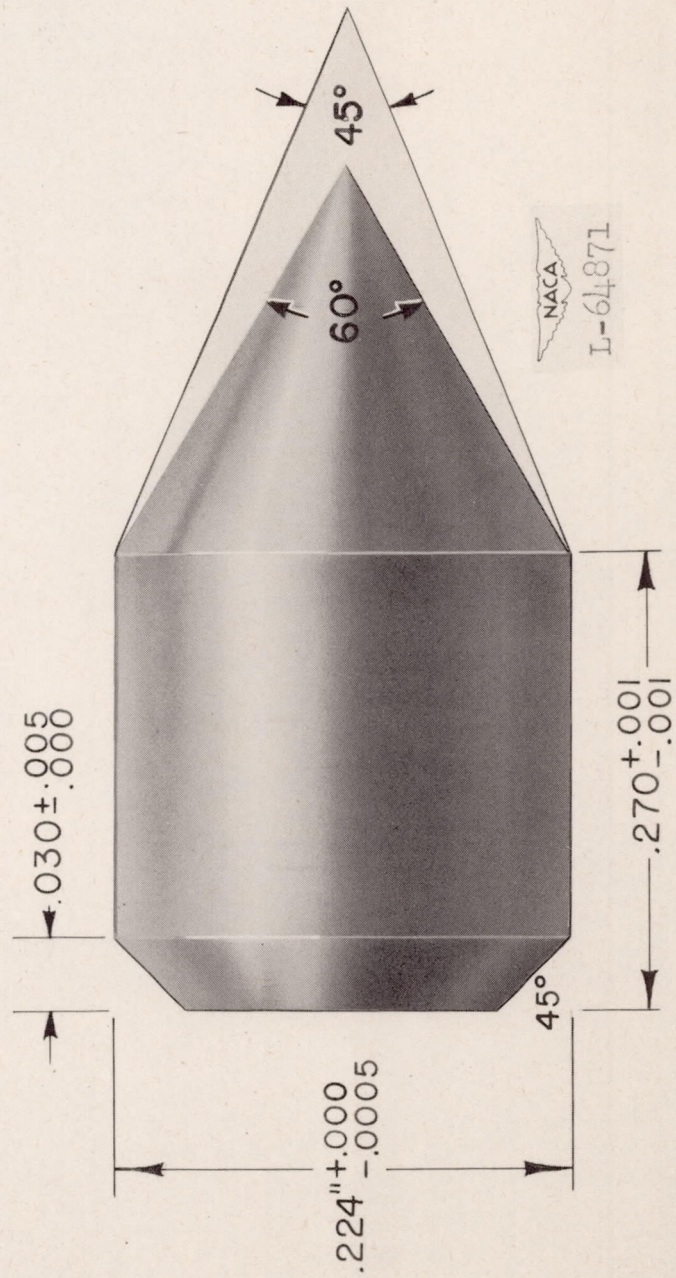
Figure 3.- Conical model detail.

C B ── Focused model

Focused shadowgraph ──

C' B' ── Lens

── Rotating mirror

D A

── Plane of model

Shadowgraph plane ──

D' A'

── Flat mirror

Parabolic mirror ──

Parabolic mirror ──

Condensing lens ──

NACA

── Light source
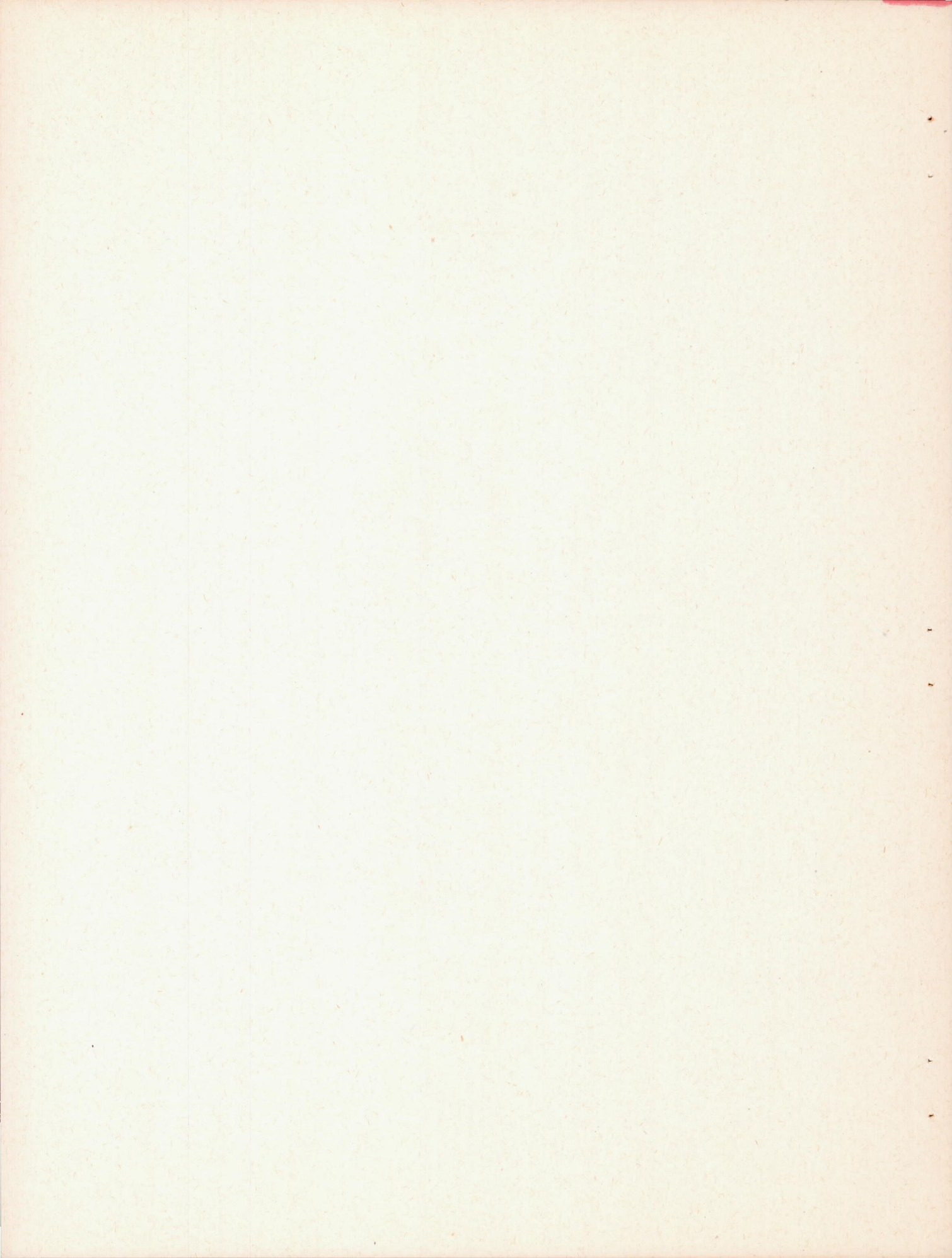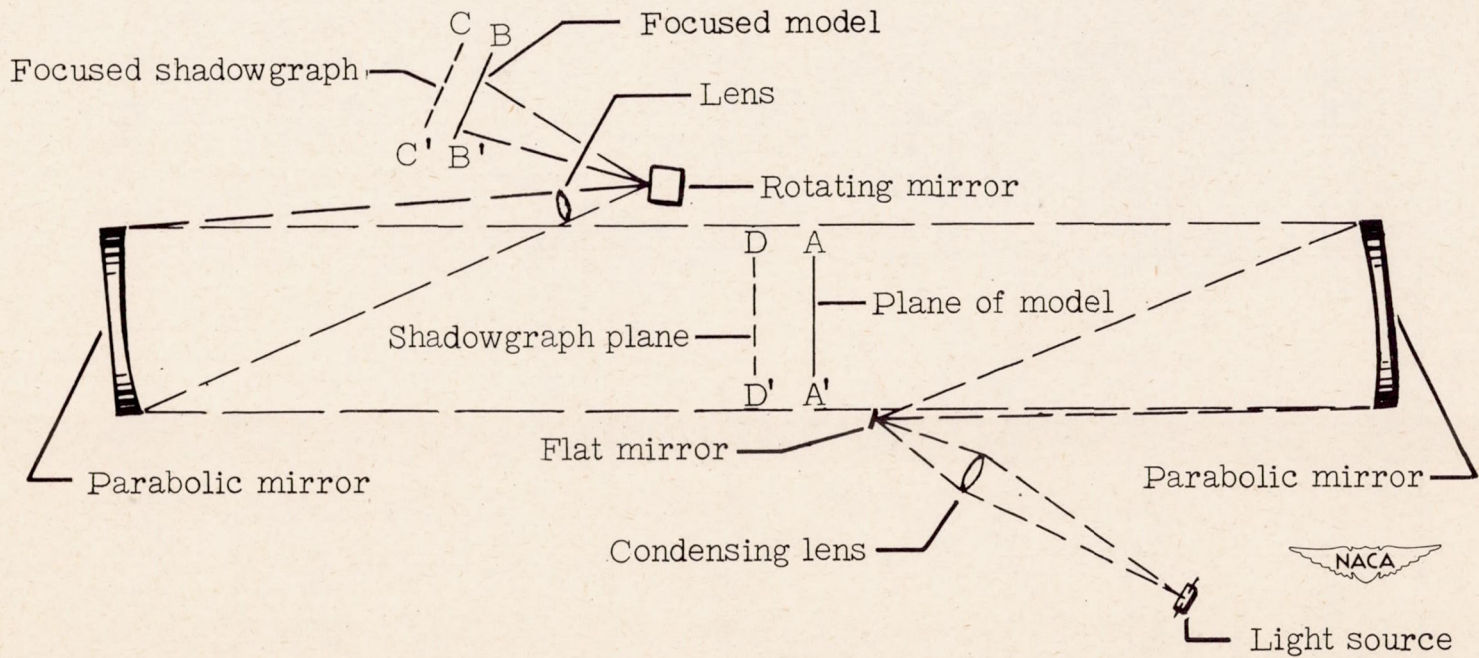
Figure 4.- Schematic representation of the focused shadowgraph system.

7.5 v, 4 amp

Selenium
rectifier
3 each in parallel

3,000 μf

12 v

1133

6 v

1 megohm, 1 w

50,000 Ω 1 w

30,000 Ω 2 w

.01 μf

B
A

.001 μf

6J6

.01 μf

1 w

929

5 megohms, 1/2

1 megohm .01 μf

5 megohms, 1/2 w

2,500 Ω 1/2 w

2,500 Ω

Screw-driver
adjustment

1 amp

5 v

5W4

250 v

250 v

6.3 v

4 μf, 450 v electrolytic

2,000 Ω, 1 w

40 μf, 450 v electrolytic

NACA
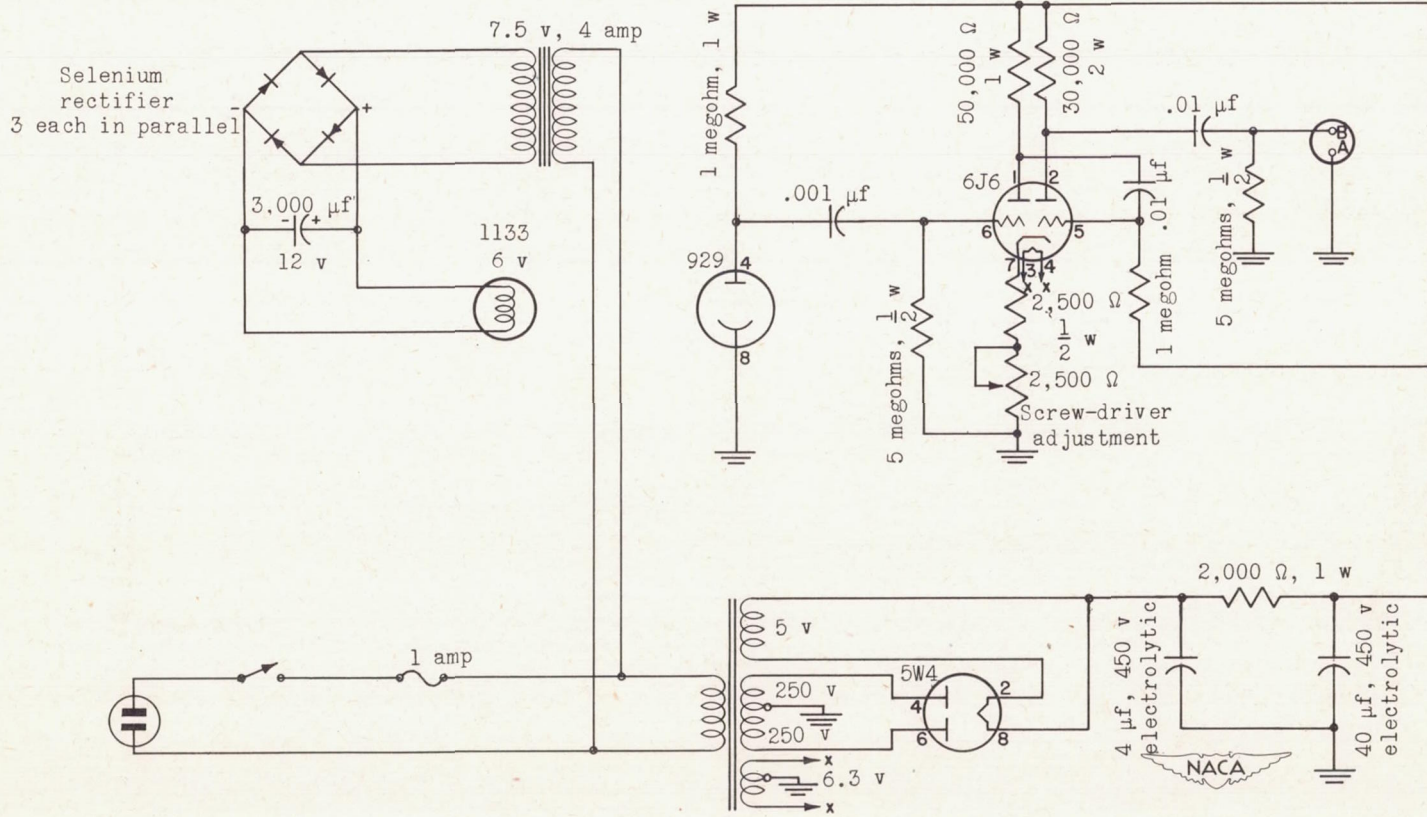
(a) Photoelectric circuit.

Figure 5.- Electronic equipment.
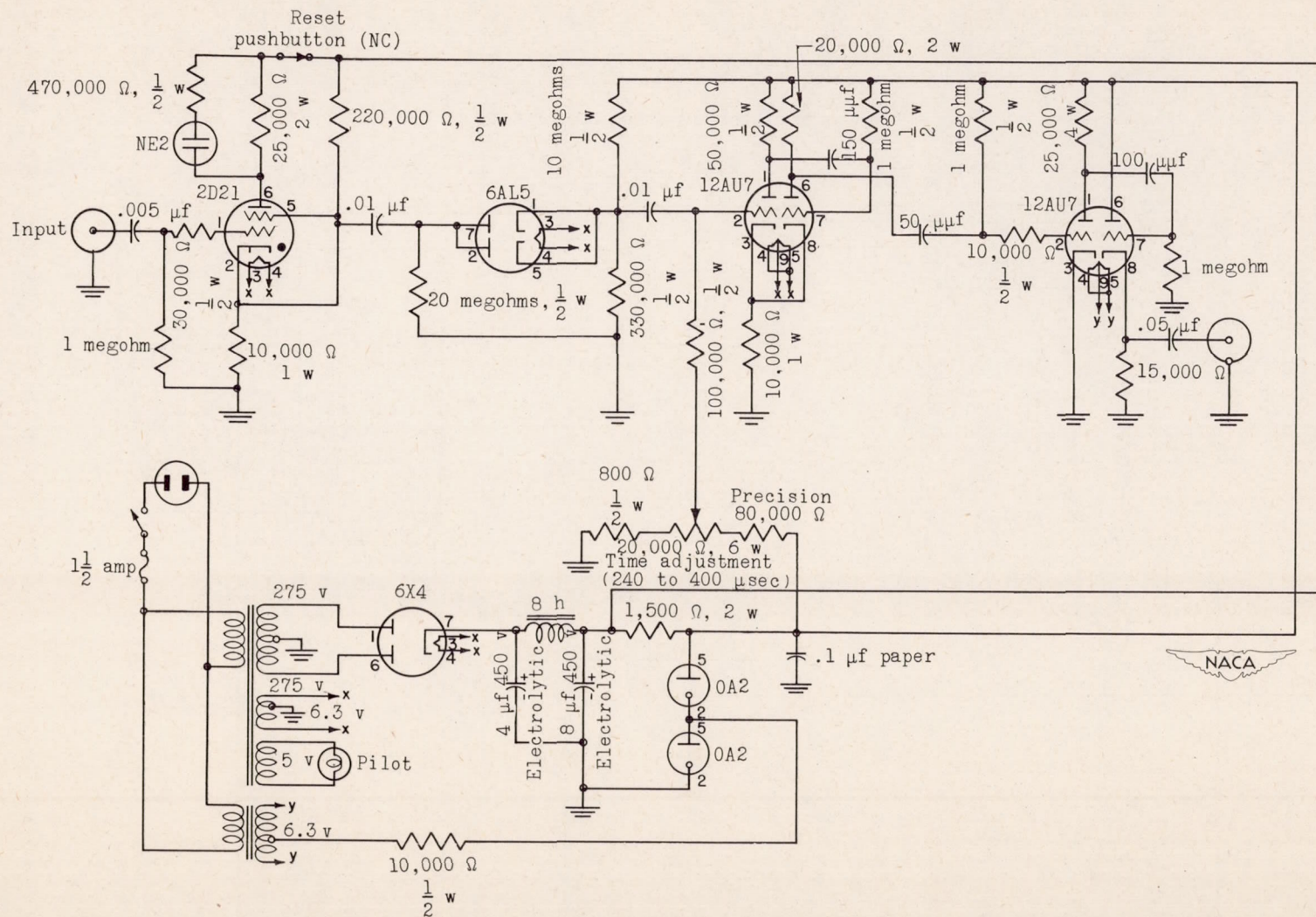
(b) Spark timing unit. Capacitors are mica unless otherwise shown.

Figure 5.- Continued.
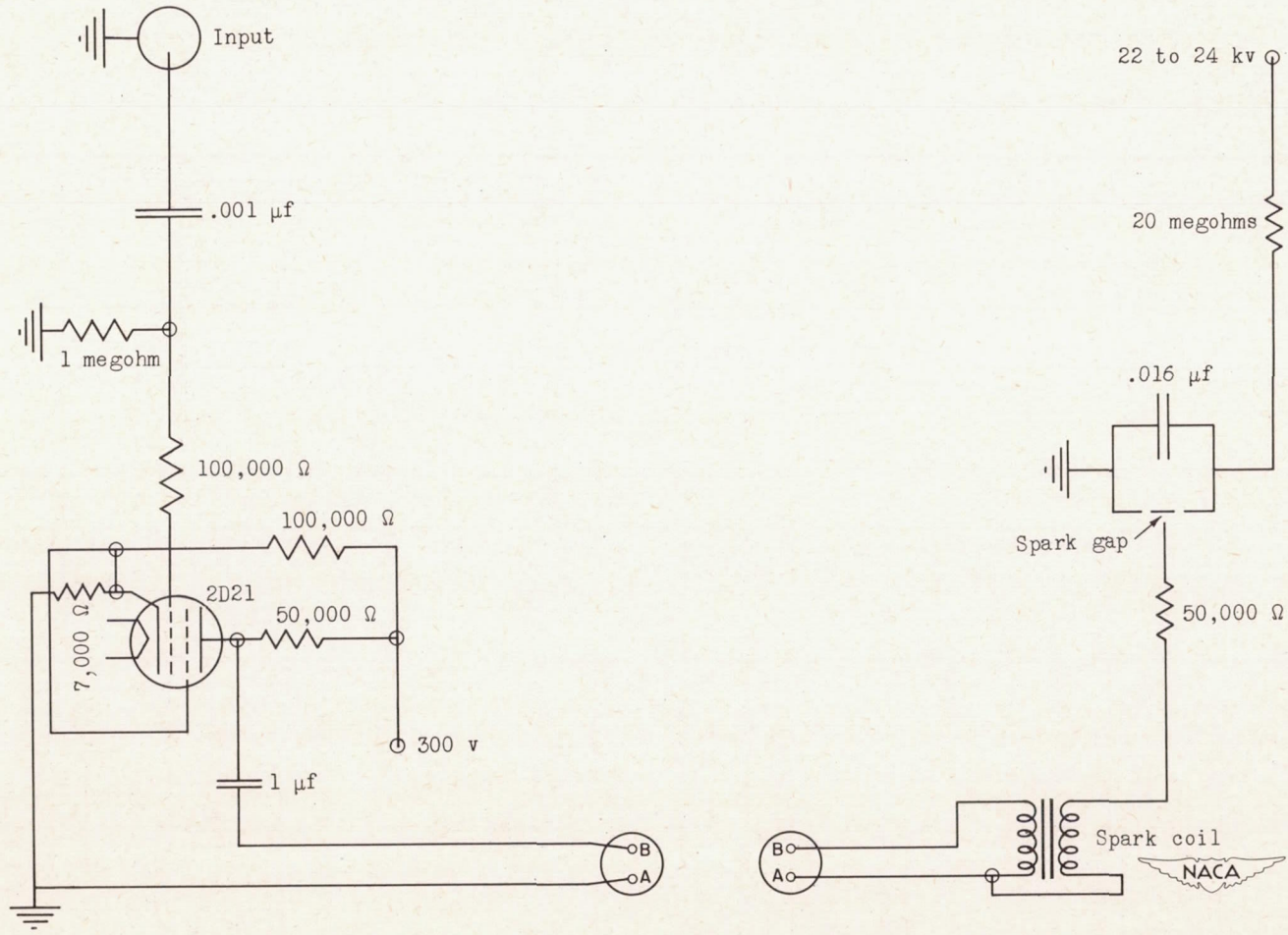
(c) Thyratron and spark circuits.

Figure 5.- Concluded.
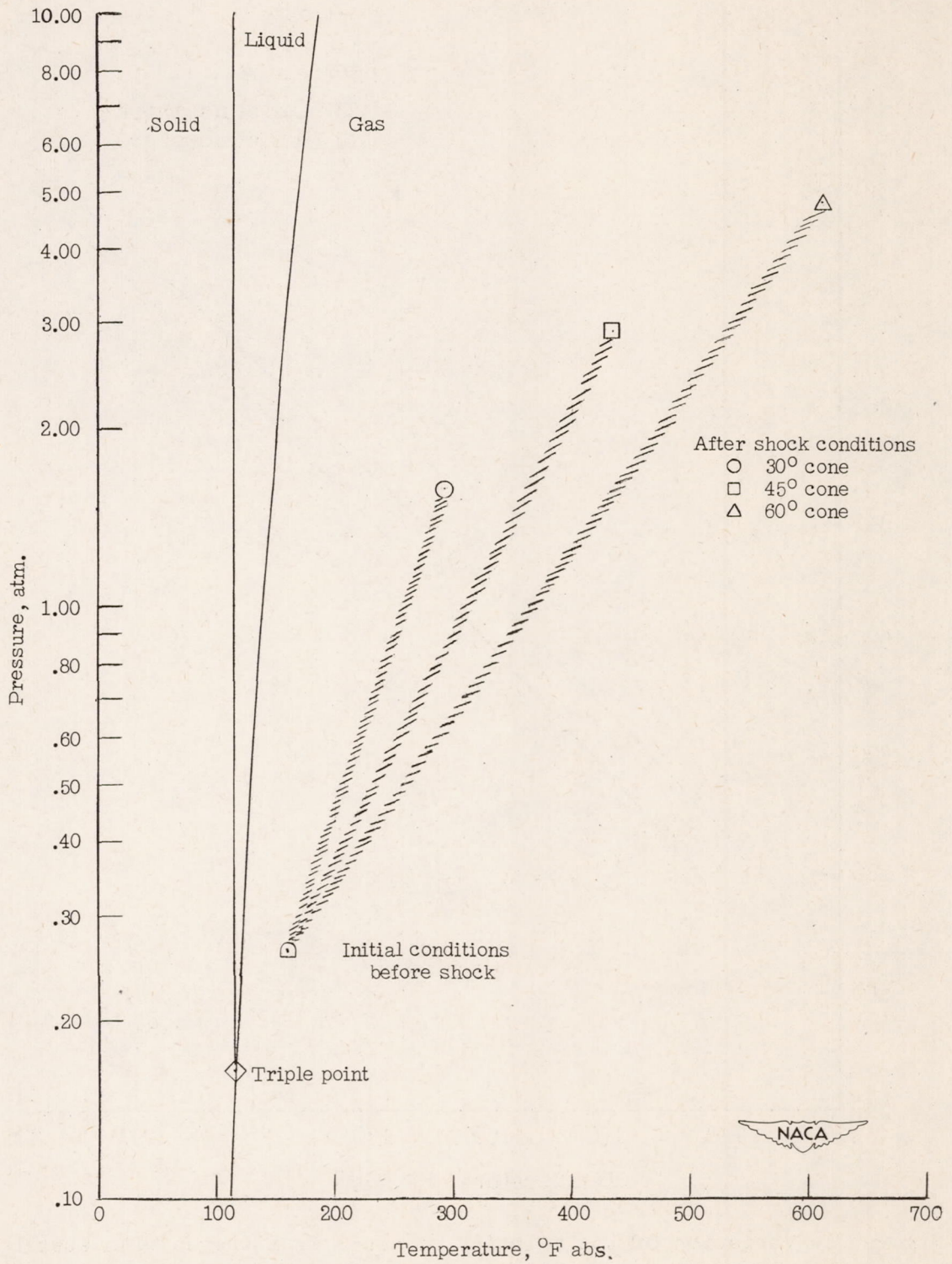
Figure 6.- Location of the initial and after shock conditions on the
nitrogen phase diagram.
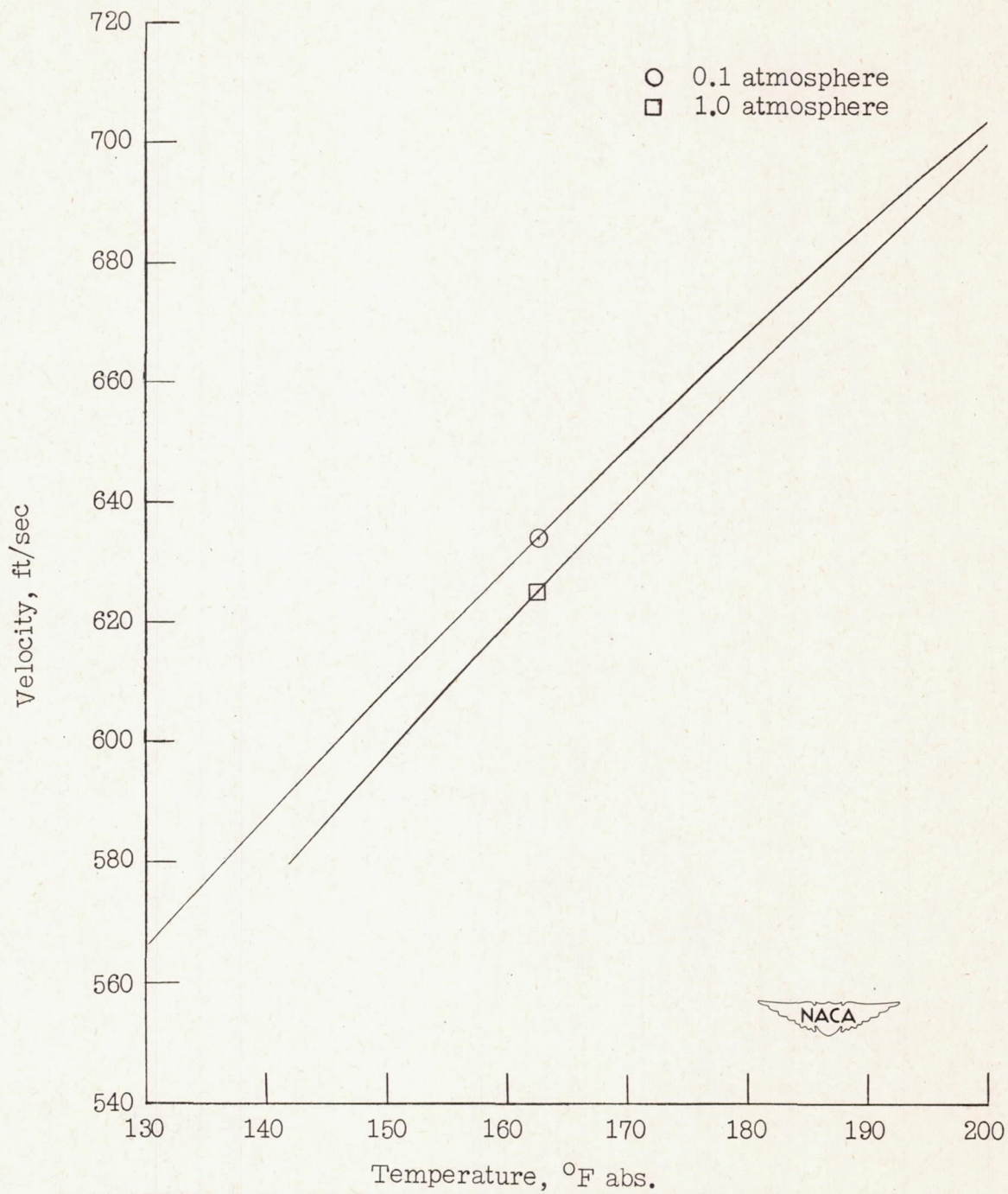
Figure 7.- Variation of the velocity of sound in nitrogen with absolute temperature. Indicated points from reference 5.
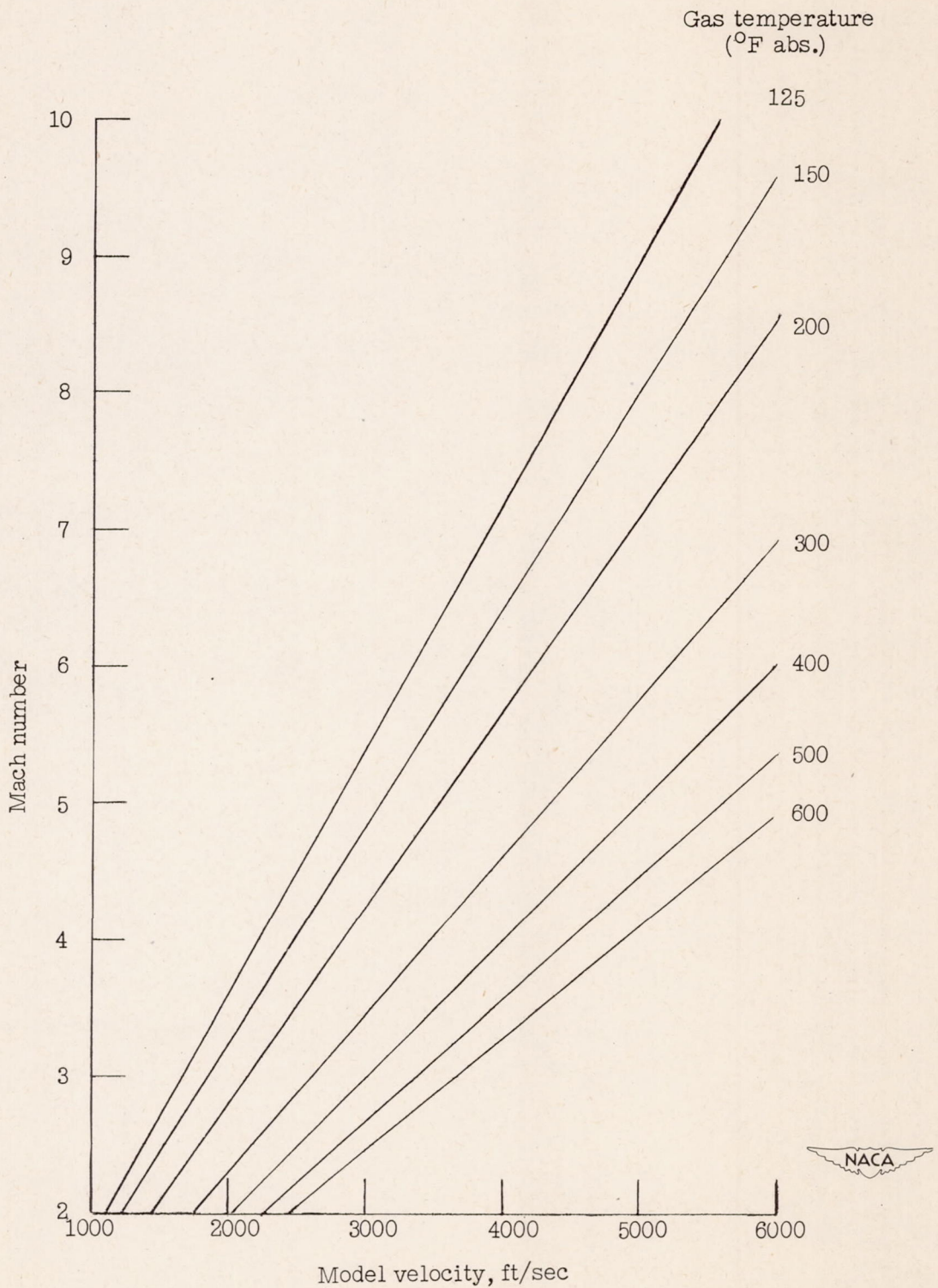
Figure 8.- Mach number, temperature, and model-velocity graph computed
by using the velocity of sound at 0.1 atmosphere in nitrogen.
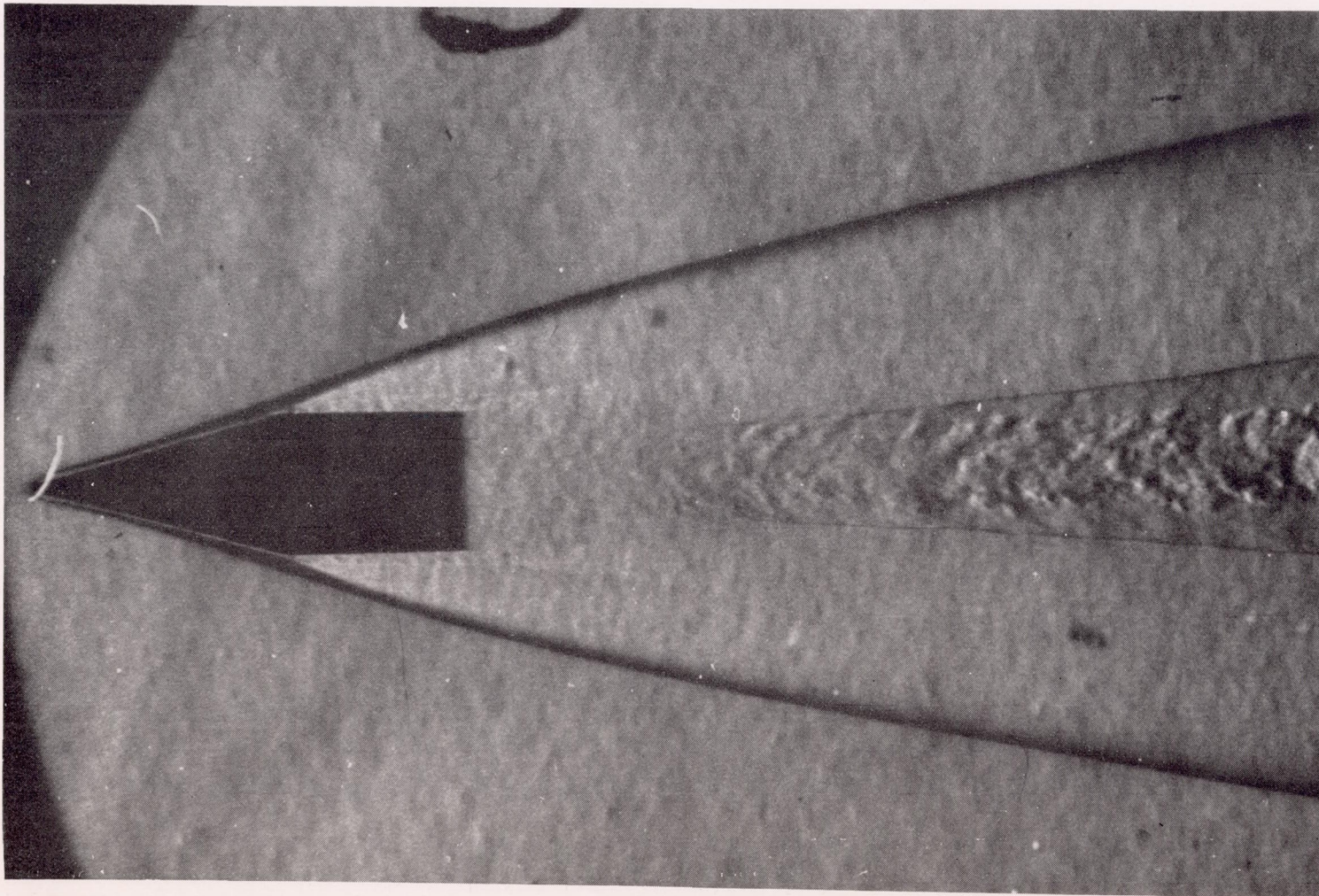
L-64867

Figure 9.- Schlieren photograph of a 30° cone having a Mach number of 6.8.
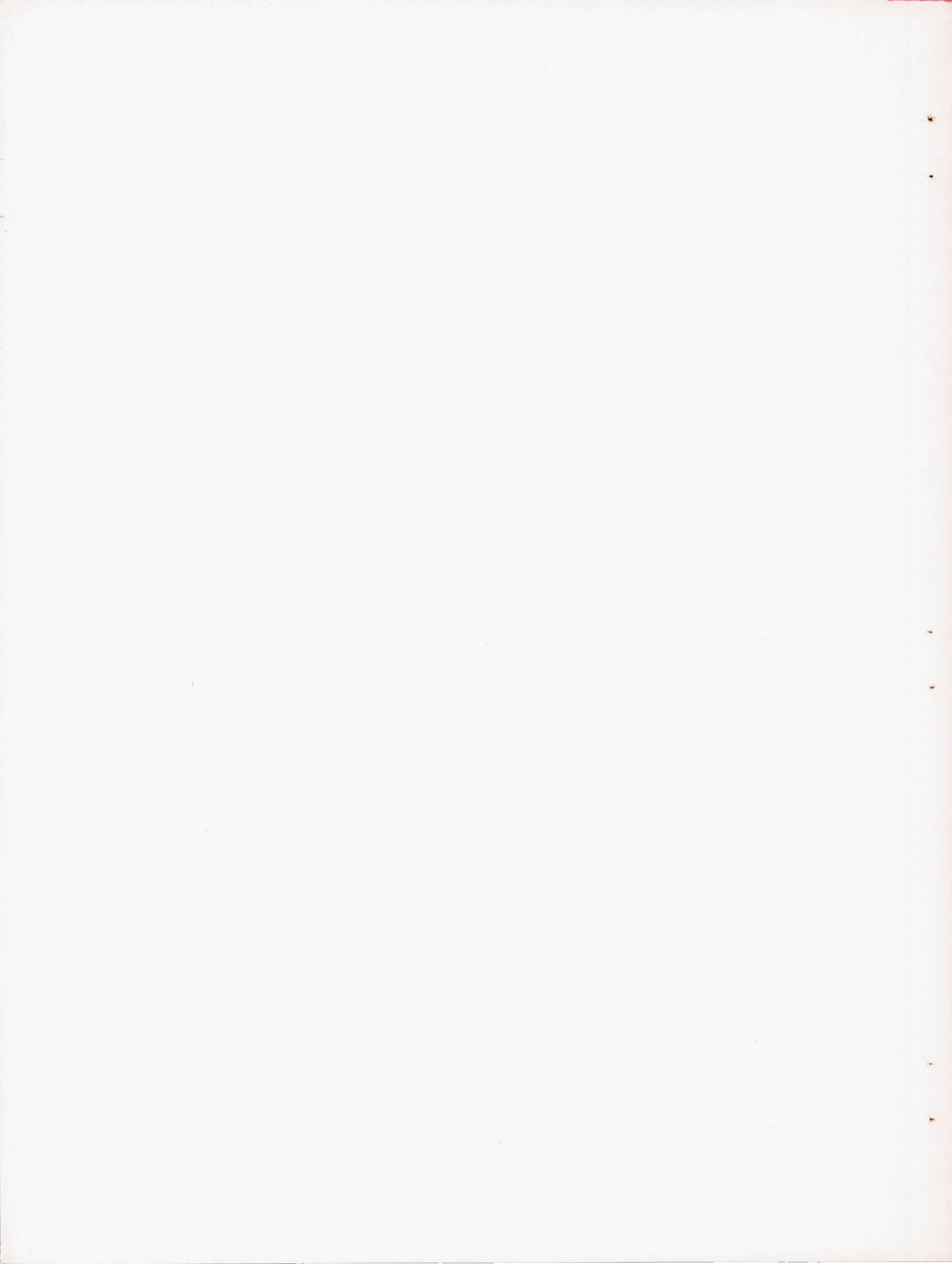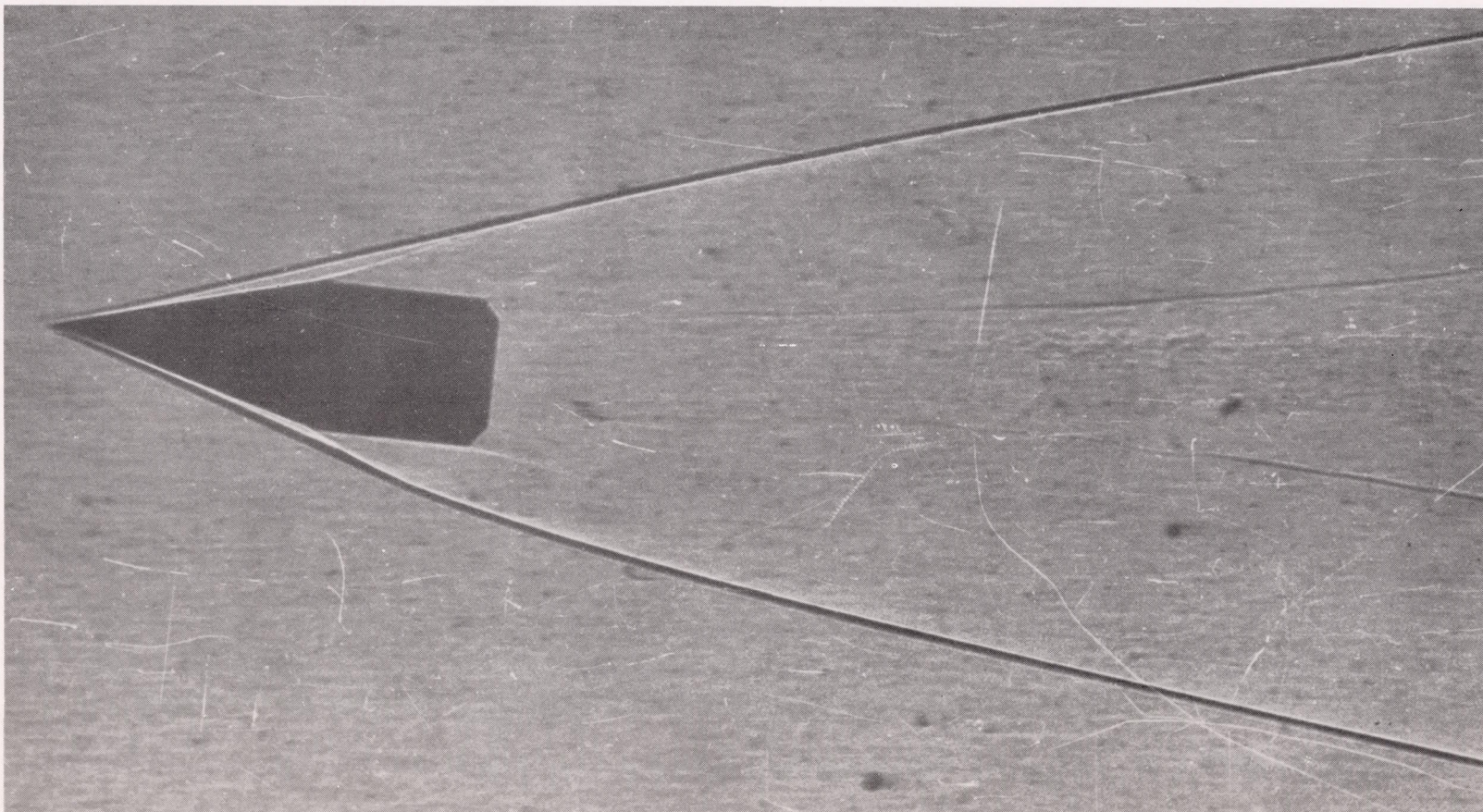
(a) 30° cone, Mach number 6.8.

L-64868

Figure 10.- Focused shadowgraphs of 30°, 45°, and 60° cones.
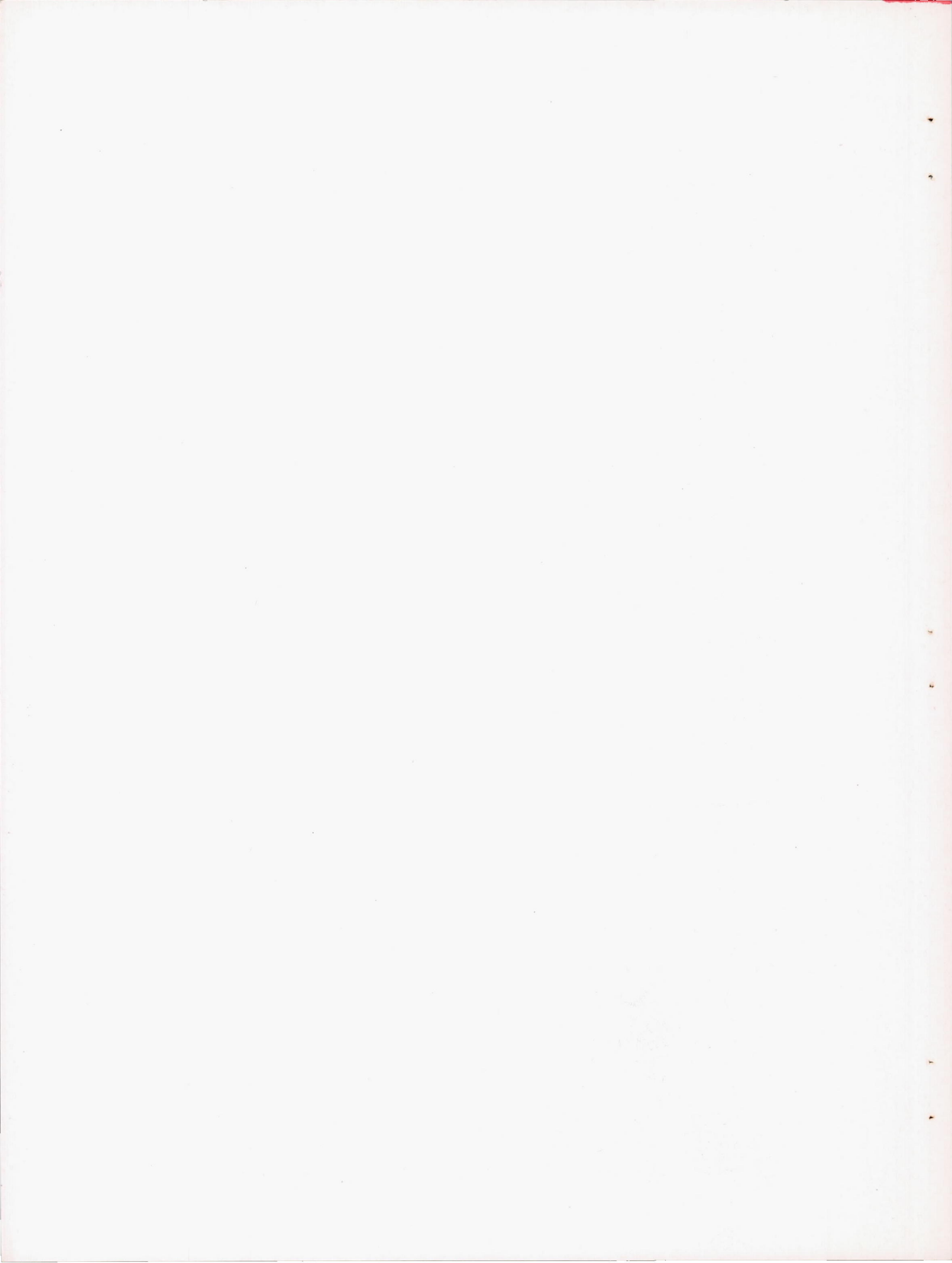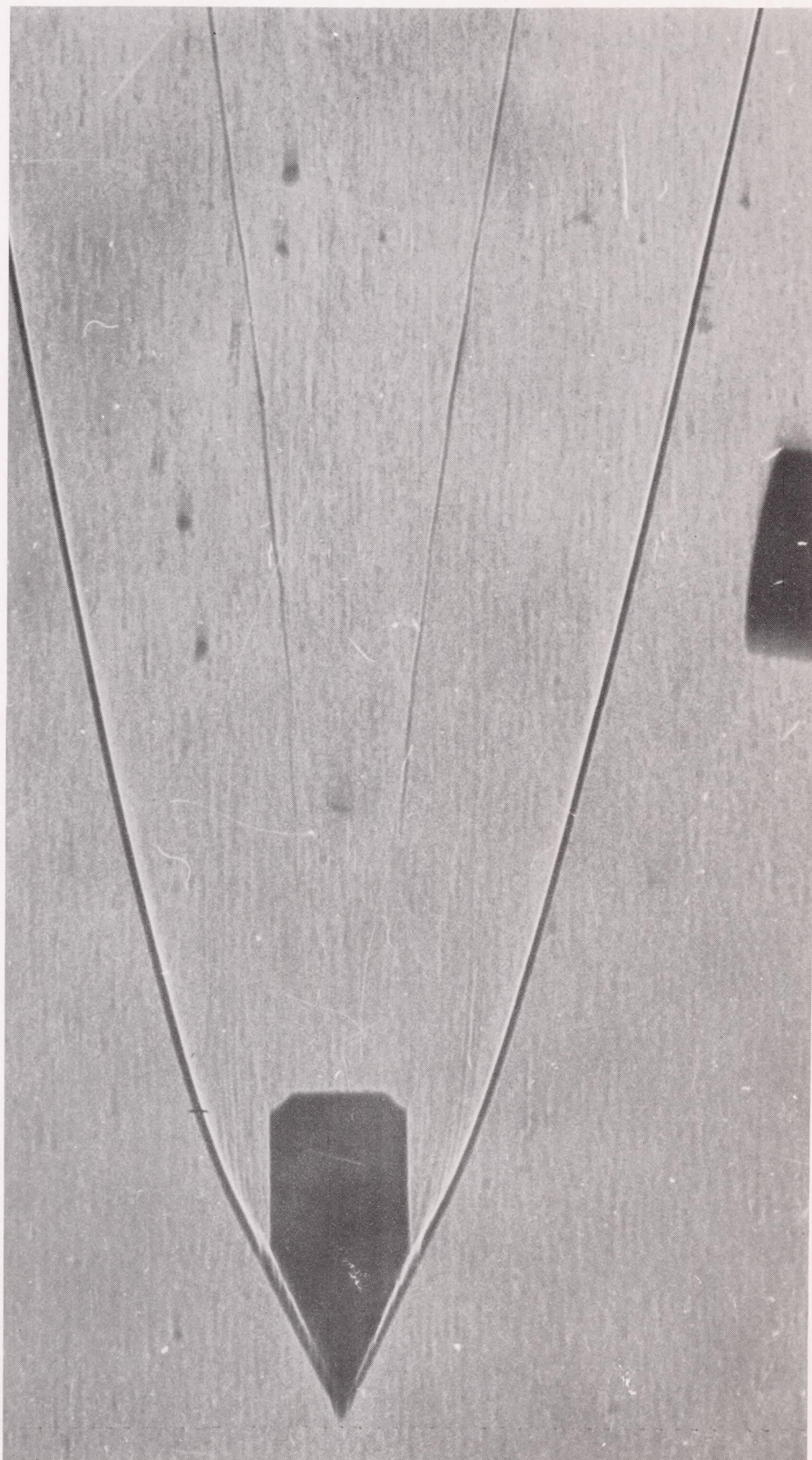
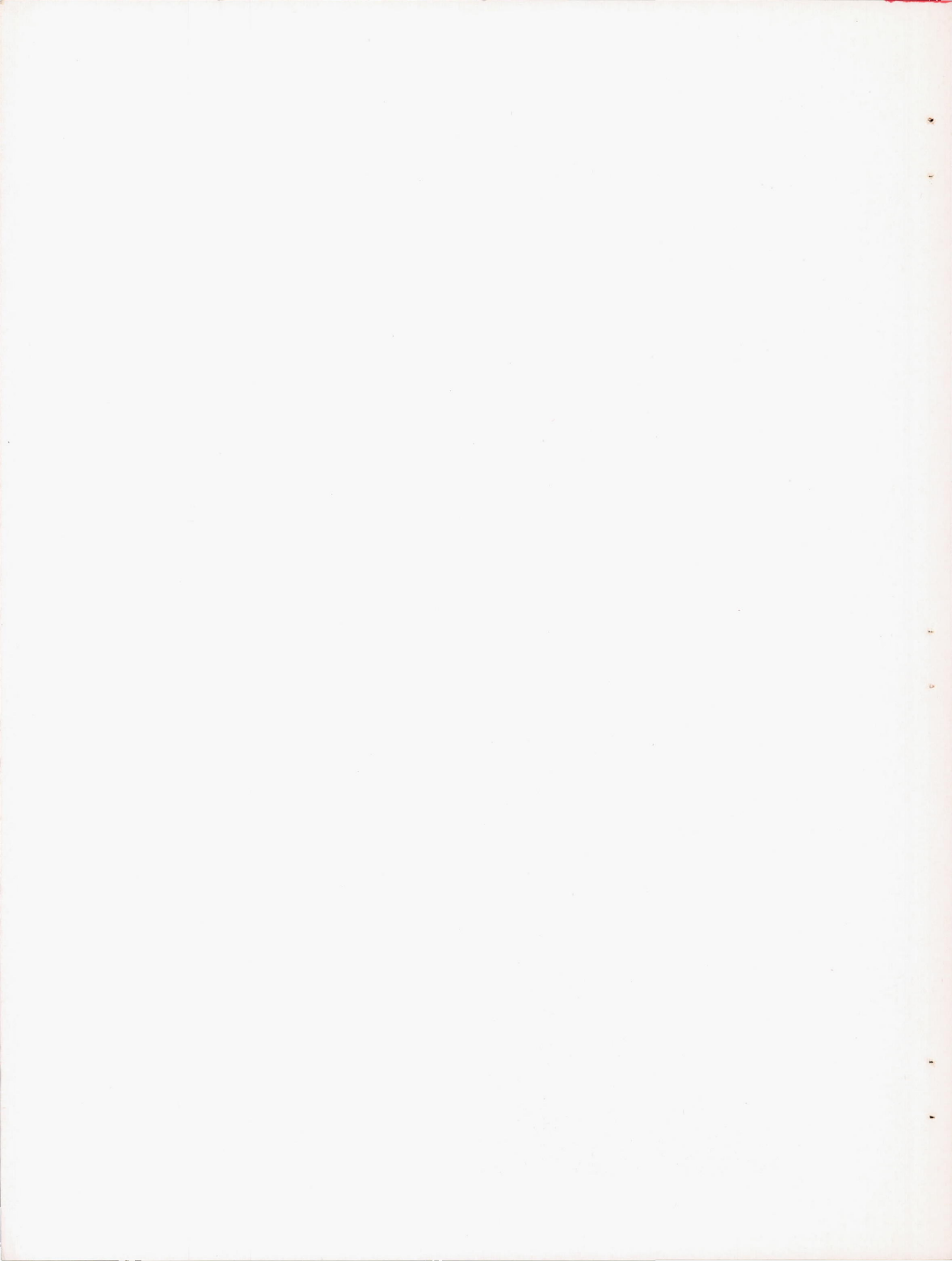(b) 45° cone, Mach number 6.6.   L-64869
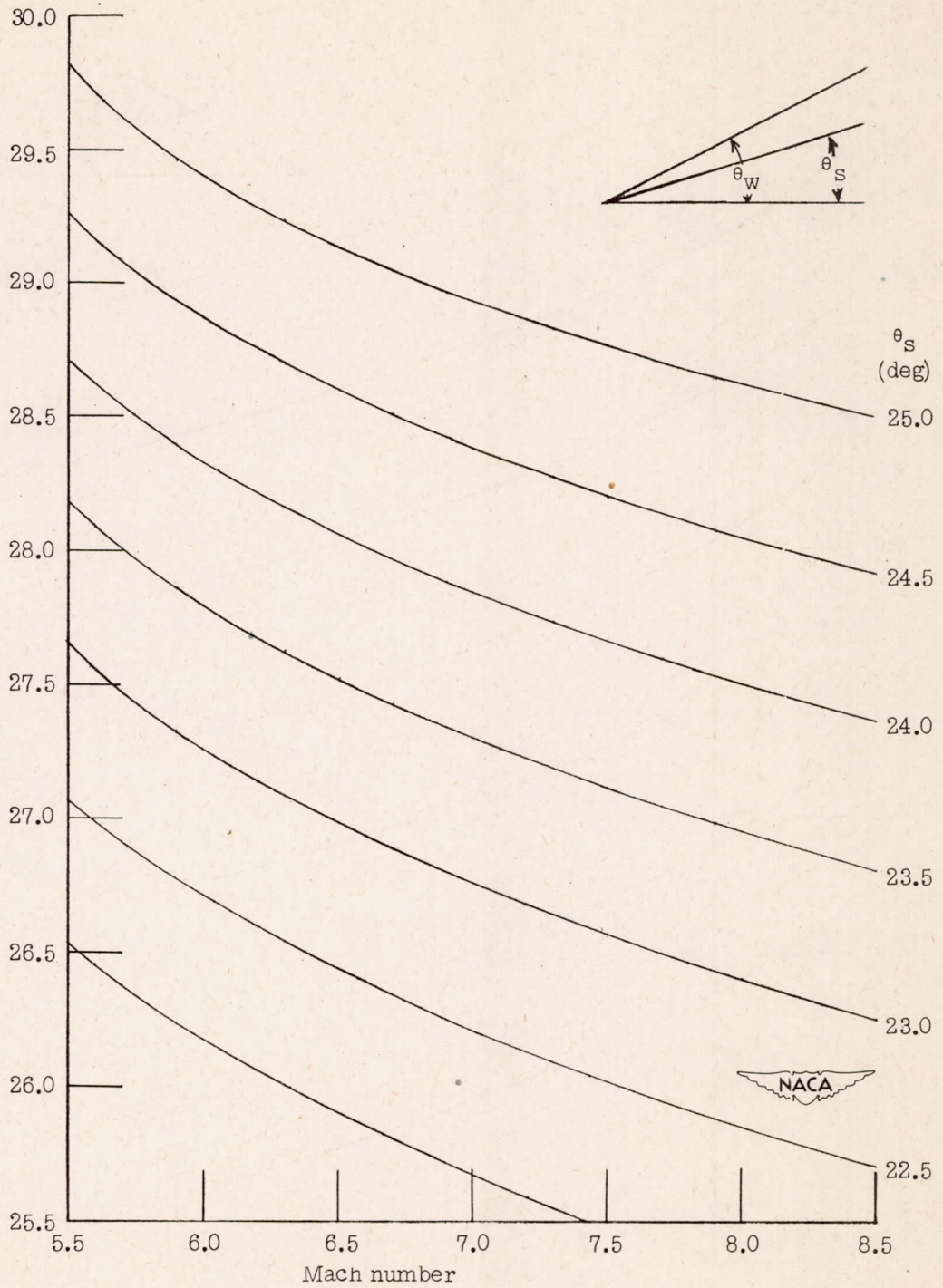
Figure 10.- Continued.
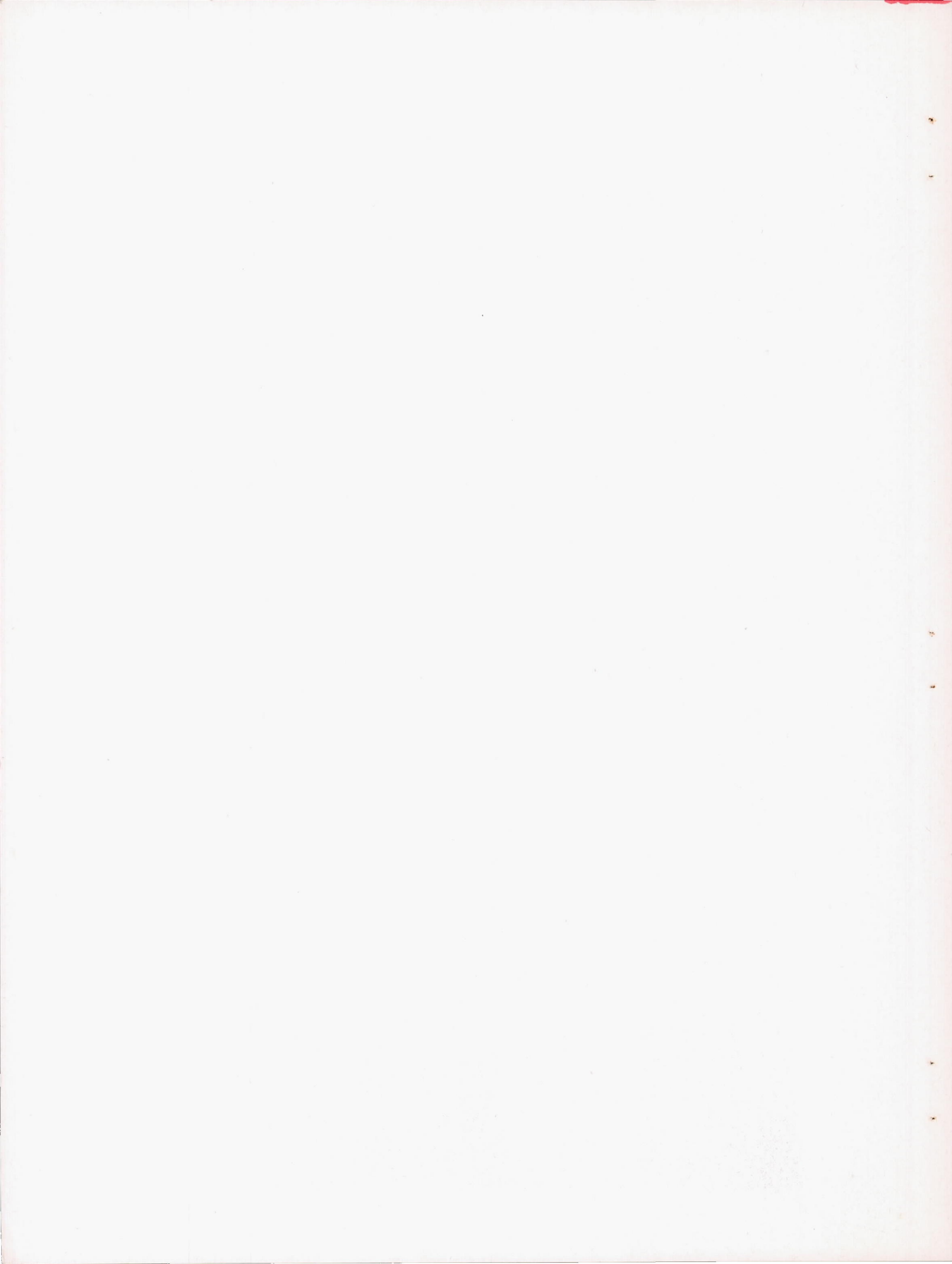
(c) 60° cone, Mach number 6.7.
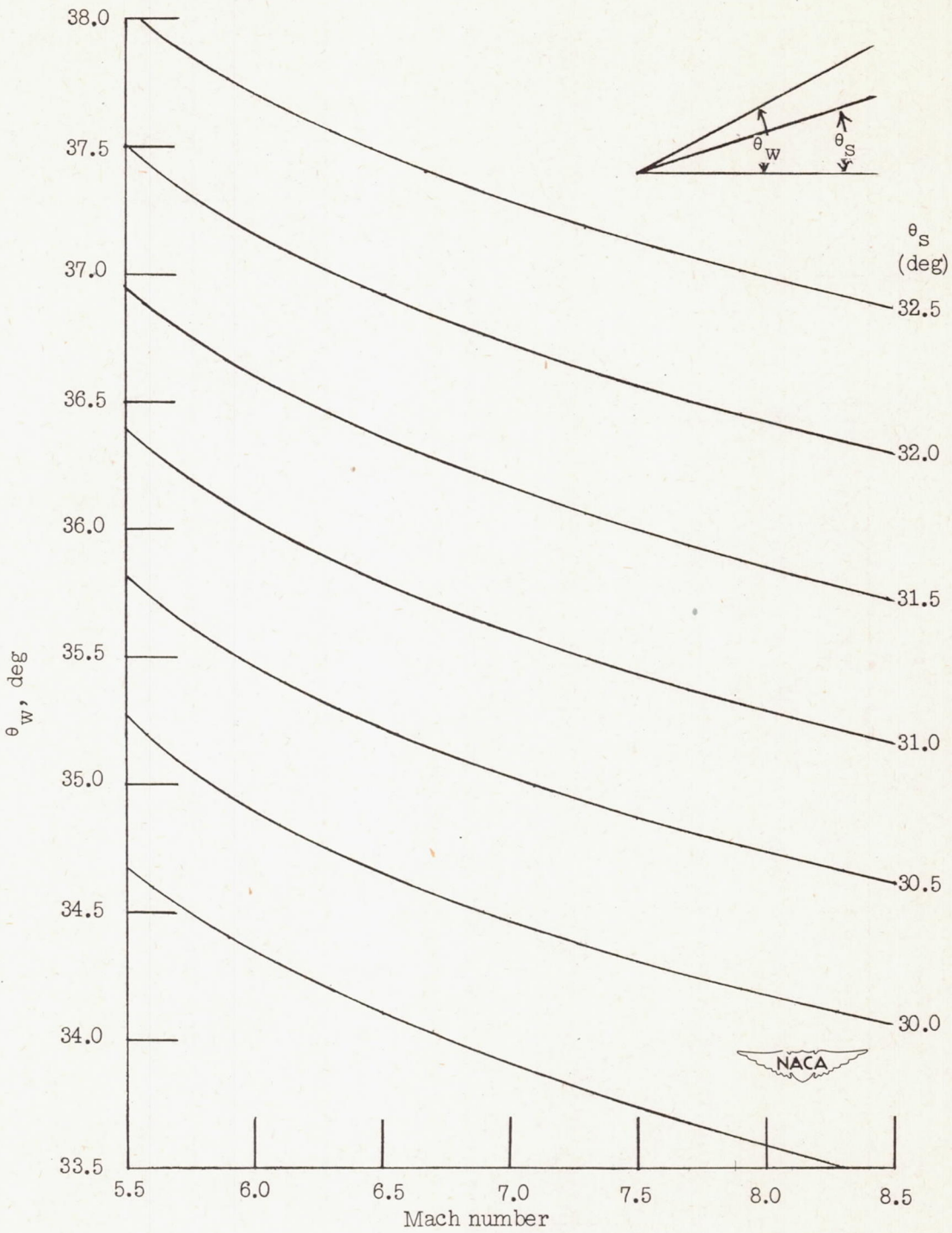
L-64870

Figure 10.- Concluded.

(a) 45° cone.

Figure 11.- Computed conical shock angles. $\gamma = 1.405$.

(b) 60° cone.

Figure 11.- Concluded.